Supporting Information

Unexpected Magnesium Oxide/Calcium Sulfide Barnacle-like Structures derived from Pyrolysed Carrageenans

Ewan D. Ward, Jolyon J. Glynn, Ryan E. Barker, Duncan MacQuarrie, and Avtar S. Matharu *

E. Ward, J. Glynn, R. Barker, D. Macquarrie, A. Matharu

Green Chemistry Centre of Excellence,

University of York, York, UK

*Email: avtar.matharu@york.ac.uk

Experimental Supplementary Information (ESI)

1. Materials and reagents

Dried and flaked Irish Moss, *Chondrus crispus*, was obtained from the Cornish Seaweed Company Ltd. Acetone was purchased from VWR chemicals. Potassium bromide (FTIR grade), potassium chloride, and sodium carbonate were purchased from Sigma Aldrich. Hydrochloric acid (37%), nitric acid (65%), sodium hydroxide, and sodium hydrogen carbonate were purchased from Fischer. Copper(II) nitrate trihydrate was purchased from Honeywell Fluka.

2. Carrageenan extraction

Dried Irish Moss biomass was ground by coffee grinder to a granular powder (<50 μm). The ground material was immersed in deionized water (25:1 mL:g) and the contents were stirred and heated to reflux for 30 minutes. The resulting gelatinous mixture was immediately centrifuged using a Thermo Fisher Megafuge 4R (3000 rpm, 30 °C, 30 min) to isolate the carrageenan containing supernatant and a sample of carrageenan supernatant was submitted for ^{1}H NMR analysis. The cooled supernatant was flash frozen in liquid N_2 and dried using a Labylo Controlled Freeze Drier for 48h or until dry (54.6 ± 3.3%).

Table X1: Characteristics of Irish Moss biomass and Irish Moss aqueous carrageenan extract

	Composition (%) [a]	
	Irish Moss Biomass (IM)	Carrageenan Extract (IME)
Proximate Analysis		
Moisture content [b]	16.4 ± 0.3	19.3 ± 0.4
Volatile content [b]	56.1 ± 0.5	51.6 ± 0.7
Fixed carbon content [b]	27.5 ± 0.1	29.1 ± 0.6
Ash content [c]	4.11	4.50
Composition Analysis:		
Carbohydrate content [d]	22.9 ± 3.2	22.3 ± 1.1
Protein content [e]	7.8 ± 0.1	N.D.
Elemental Analysis:		
C	29.4 ± 0.04	25.4 ± 0.05
H	4.8 ± 0.16	4.3 ± 0.01
N	2.19 ± 0.03	N.D.
S	1.56 ± 0.09	4.9 ± 0.17
O	57.9 ± 0.32	60.9 ± 0.23

[a] Wet basis [b] Derived via TGA [c] ICP-MS [d] Acid digestion & HPLC

[e] 3.55x N content [f] by difference (O = 100 – C – H – N – S – Ash)

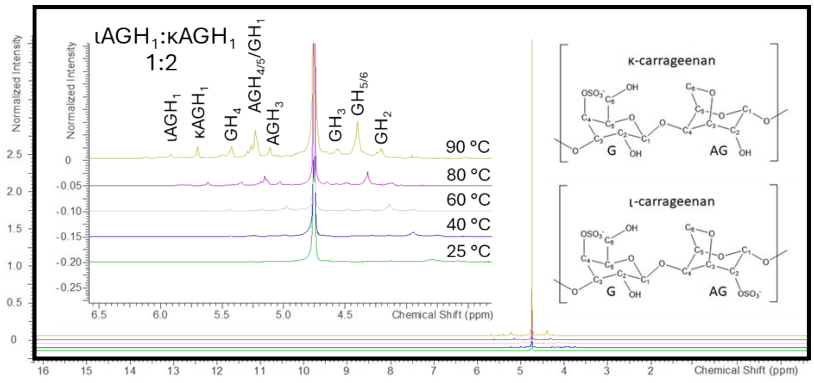

Figure X1 Overlaid VT (20 to 90 °C) 500 MHz ^{1}H NMR spectroscopy of extracted carrageenan in D_2O. Assigned as carrageenan (structure inset), specifically noting anomeric anhydrogalactose protons between 5.75 and 6.00 ppm of both iota and kappa carrageenan.

3. Characterisation of char materials

Char samples were characterised via the following:

a) **Elemental analysis** of the chars were performed via CHN microanalysis using an Exeter Analytical Inc CE440 analyser. Sulfur content was determined via oxygen combustion and subsequent sulfate analysis using a Thermo scientific Dionex Aquion Ion chromatography system (Dionex IonPac AS22 RFIC 4 x

250 mm column). Mineral content was calculated using an Agilent 7700 series ICP-MS following sample digestion in nitric acid and hydrogen peroxide.

b) **Thermogravimetric analysis (TGA)** was performed using a Netzsch 409 Thermal Gravimetric Analyser. The samples (~50 mg) were heated under nitrogen (100 mL min^{-1}) from 20 °C to 1000 °C (10 K min^{-1}) and held for 20 min.

c) **Powder X-ray Diffraction** was performed on a Panalytical Aeris Powder XRD to recognise and identify salt content. Finely ground sample was packed into a 2.5 cm diameter sample holder at a depth of approximately 1 mm. A scan from 5° to 100° 2Θ was performed at a rate of 0.02° sec^{-1}.

d) **^{13}C cross polarisation magic angle spinning (CPMAS) SSNMR** spectroscopy was performed on a 400 MHz Bruker Avance III HD spectrometer with a spin rate of 10,000 Hz, recycle delays of 5 s, a total number of 512 scans.

e) **FT-IR spectroscopy** was performed using a Perkin-Elmer Spectrum Two FT-IR spectrometer of sample disks: finely ground and dry sample diluted in potassium bromide (0.5% (w/w)) and compressed under vacuum (Specac Manual Hydraulic Press).

f) **X-ray photoelectron spectroscopy (XPS)** was used to determine the chemical states of sulfur and carbon within the chars, and to also measure magnesium and copper content at the surface. XPS was performed using a Kratos Axis Ultra DLD system and monochromatic Al Ka X-ray source operating at 144 W (12 mA x 12 kV). High-resolution scans with pass energies of 20 eV and step sizes of 0.1 eV were taken of samples mounted into an 8 mm diameter well of a modified standard Kratos sample bar.

g) Macromolecular structure was determined using **high resolution transmission electron microscopy (HRTEM)**, which was performed using a Jeol 2100, 200kV Field Emission Transmission and Scanning Transmission Electron Microscope. Samples suspended to a lacey carbon film on 200 Mesh Copper grid were imaged at magnifications of x50k to x500k.

h) Topography and morphology of the char particles were determined using **scanning electron microscopy (SEM)** were performed using a Jeol JSM-7800F Schottky field emission scanning electron microscope (15 kV A.V, 10 mm W.D) images between x1k and x100k magnification were taken. Elemental composition was determined via the insertion of Dual Oxford Instruments large area solid state detectors for **energy dispersive X-ray spectroscopy (EDX)**. Before imaging samples were loaded onto an aluminium stub via carbon tape and coated using a Jeol JFC-2300HR fine coater and FC-TM20 thickness controller to coat with 5nm of Pd/Au at a current of 80 mA.

i) Pore characterisation was performed using **N_2 Adsorption porosimetry** isotherms which were recorded on a Micromeritics Tristar II porosimeter at 77 K of ground degassed samples (30 mbar, 120 °C for 20 h).

j) **PZC analysis** was performed by pH drift measurements. Samples (50 mg) were added to 20 mL of degassed pH solution (pH 1-12; achieved by appropriate mixing of potassium chloride solution (0.1 M); hydrochloric acid (0.1 M), and sodium hydroxide (0.1 M)) after 24h the pH drift was measured using a calibrated pH probe (Jenway model 6505).

k) **Boehm titrations** were performed according to Shannon [1]. Test material (0.5 g) was added to solutions of NaOH, $NaHCO_3$, Na_2CO_3, and HCl (25 mL, 0.05 M) and agitated for 12h. The resulting mixture was filtered and divided into five equal aliquots. For the basic solutions, each aliquot was acidified with 0.05

M HCl, basified with an excess of NaOH (0.05 M) before and back titrated with HCl (0.05 M). For acid solutions an equivalent methodology was used. Titrations were conducted with a 907 titrando auto titrator with an 804 titrando stirrer set up and using a set endpoint pH (pH 4 or 10). A first titration would be set (±1 from endpoint pH) with an addition rate of 0.1 ml/min following a second titration (endpoint pH 7.1) with a slow addition (0.10 µl per min).

l) **Zeta potential** values were measured using Smoluchowski method [2] in triplicate by a Malvern Panalytical Zetasizer Nano. Solutions of approximately pH 3, 5, 7, and 9 were achieved by mixing appropriate amounts of potassium chloride solution (0.1 M); hydrochloric acid (0.1 M), and sodium hydroxide (0.1 M)). Into 1 mL of each solution approximately 5 mg of sample material was immersed and shaken before being transferred into a Malvern Panalytical folded capillary cell.

4. Acid washing of chars

Acid washing was performed to further understand the char characteristics. These chars underwent dispersion in 25:1 (v:w) 1 M aqueous HCl and were agitated for 48h. The chars were filtered and washed with distilled water to remove excess acid, and dried.

5. Copper(II) Adsorption

The Adsorption capacity was determined as described in the manuscript and a calibration curve of UV-vis absorbance intensity at 810 nm vs copper(II) concentration (aqueous). Two adsorption isotherm models were applied, Langmuir and Freundlich. The Langmuir isotherm model assumes monolayer formation on a homogeneous surface and indicates a saturated coverage [3]. The Langmuir equation is written below in E1 and the linearised form in E2:

$$q_c = \frac{q_m K_L C}{1 + K_L C} \quad \text{(E1)}$$

$$\frac{1}{q_c} = \frac{1}{q_m} + \frac{1}{q_m K_L} \cdot \frac{1}{C} \quad \text{(E2)}$$

Where q_c is the measured adsorption capacity at concentration, C, q_m is the maximum adsorption capacity, and K_L is the Langmuir constant. The Freundlich isotherm, on the other hand, is applicable to multilayer adsorption on heterogeneous surfaces [4]. The Freundlich equation is written below in E3 and the linearised form in E4:

$$q_c = K_F C^{1/n} \quad \text{(E3)}$$

$$\log(q_c) = \log(K_F) + \frac{1}{n} \cdot log(C) \quad \text{(E4)}$$

Where, once again, q_c is the measured adsorption capacity at concentration, C, K_F is the Freundlich coefficient, and n is the Freundlich constant.

Applying a kinetic order model enables the metal adsorption mechanism and rate controlling steps to be estimated. The most widely used kinetic models are the pseudo-first order (E5) and pseudo-second order models (E6). Linearised forms are shown in E7 and E8, respectively [5].

$$\frac{dq_t}{dt} = k_1 \cdot (q_e - q_t) \quad \text{(E5)}$$

$$\frac{dq_t}{dt} = k_2 \cdot (q_e - q_t)^2 \quad \text{(E6)}$$

$$\ln(q_e - q_t) = \ln(q_e) - k_1 \cdot t \quad \text{(E7)}$$

$$\frac{t}{q_t} = \frac{1}{k_2 q_e^{\,2}} + \frac{1}{q_e} \cdot t \quad \text{(E8)}$$

Where q_t is the adsorption capacity at time, t, q_e is the adsorption capacity at equilibrium (in the pseudo-first order model equilibrium was assumed to be met after 24 h), and k_1 and k_2 are the rate constants for the pseudo-first and second order models, respectively.

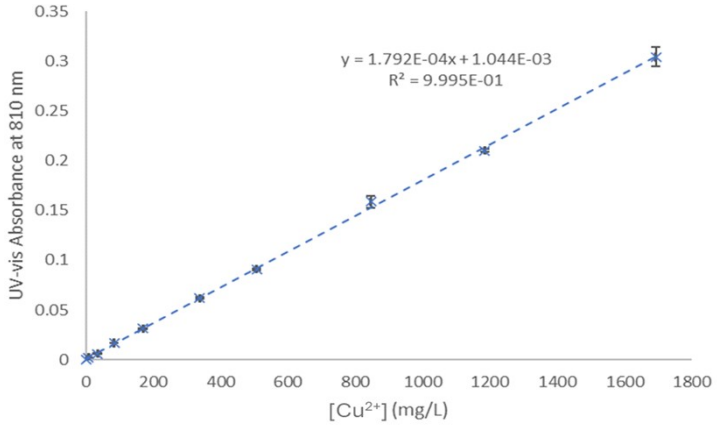

Figure X3 - UV-vis Calibration curve indicating the effect of copper(II) concentration on the absorbance intensity at 810 nm.

Supplementary figures

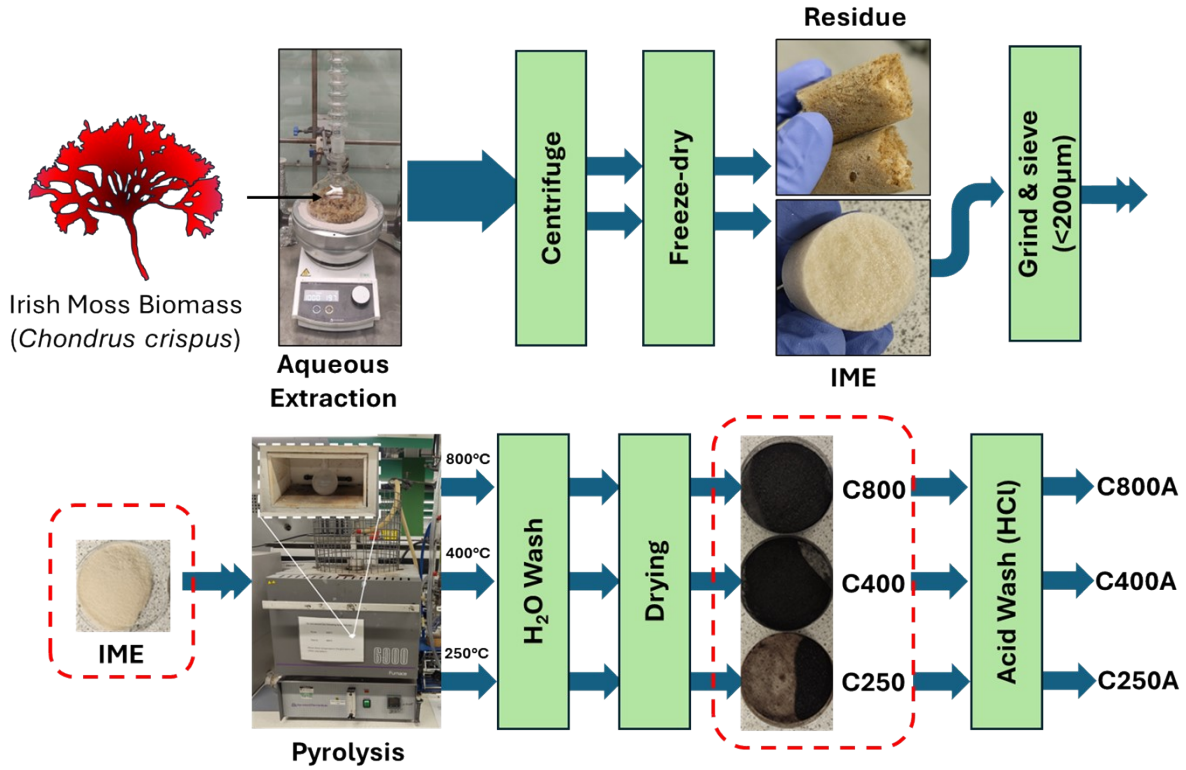

Figure S1 – Flow chart process depicting C250-C800 production. Images of the initial carrageenan aerogel and subsequent chars: C250, C400, and C800 are highlighted.

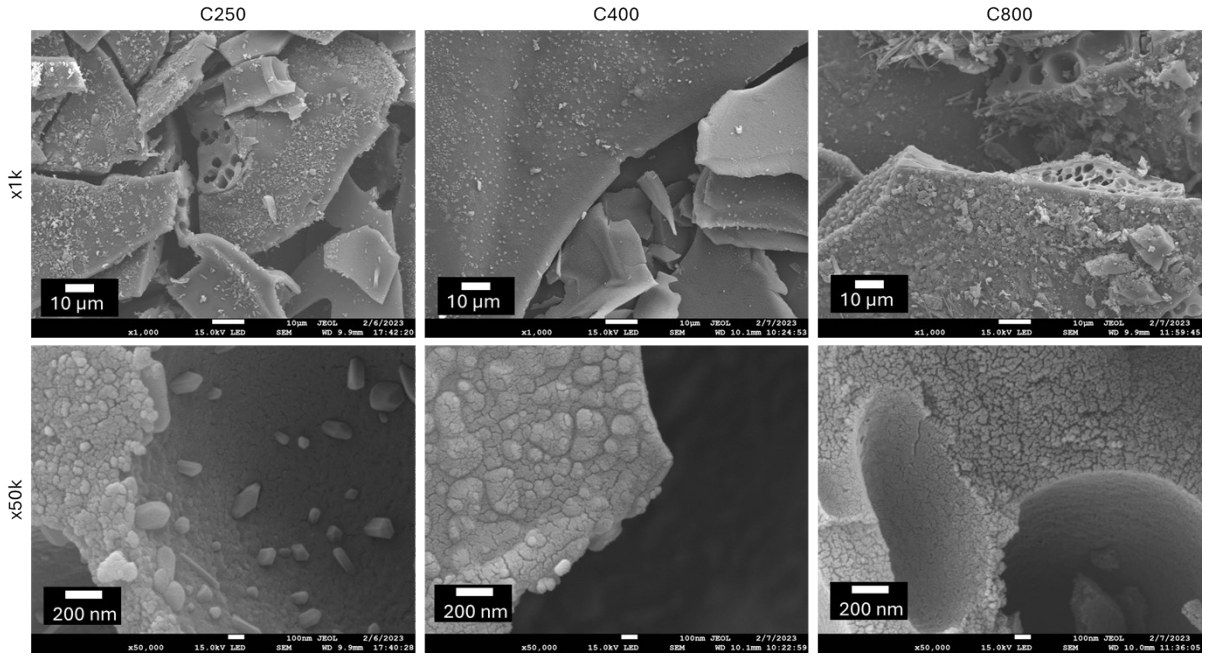

Figure S2 – SEM images of Pd/Au coated (5 nm) unwashed C250-C800 at magnifications of x1k and x50k

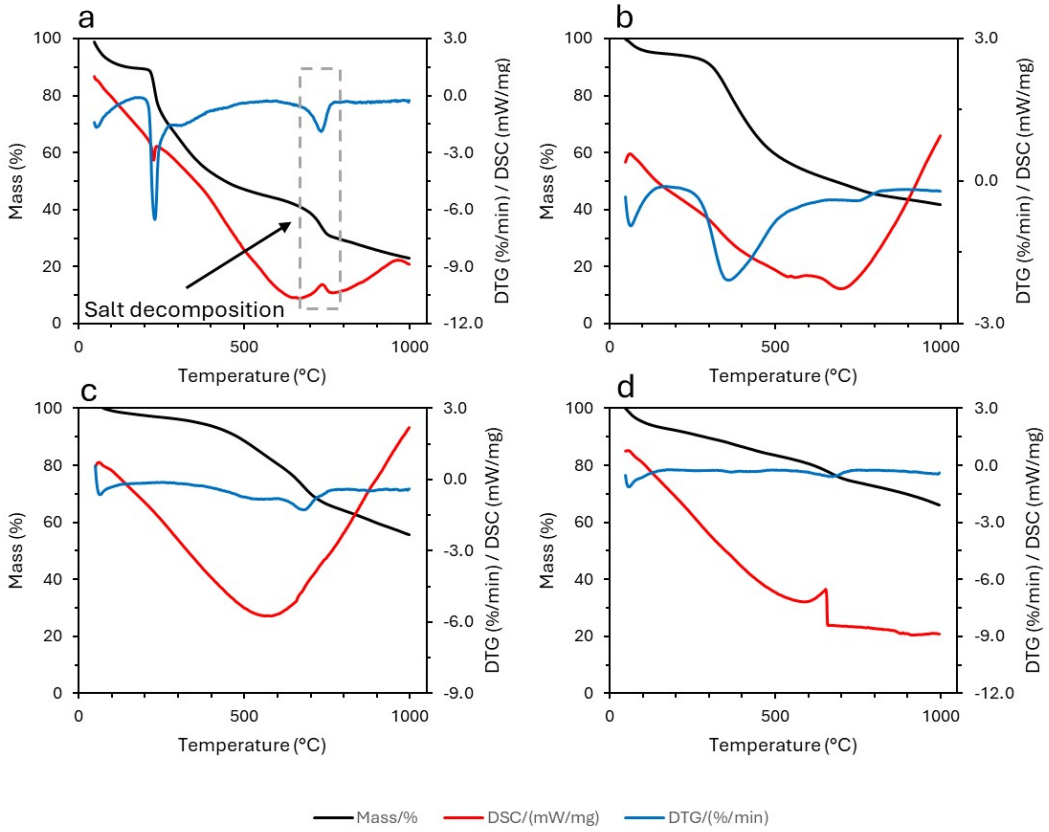

Figure S3 – TG (black line), DTG (blue line), and DSC (red line) thermograms of a) the initial carrageenan extract (IME), and the subsequent chars b, c, and d) C250, C400 and C800, respectively.

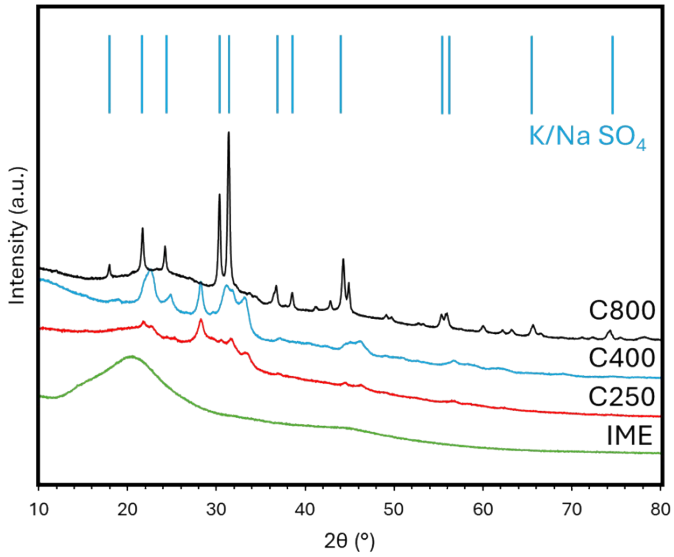

Figure S4 - pXRD diffractograms of unwashed carrageenan chars highlighting sodium/potassium sulfate diffraction planes.

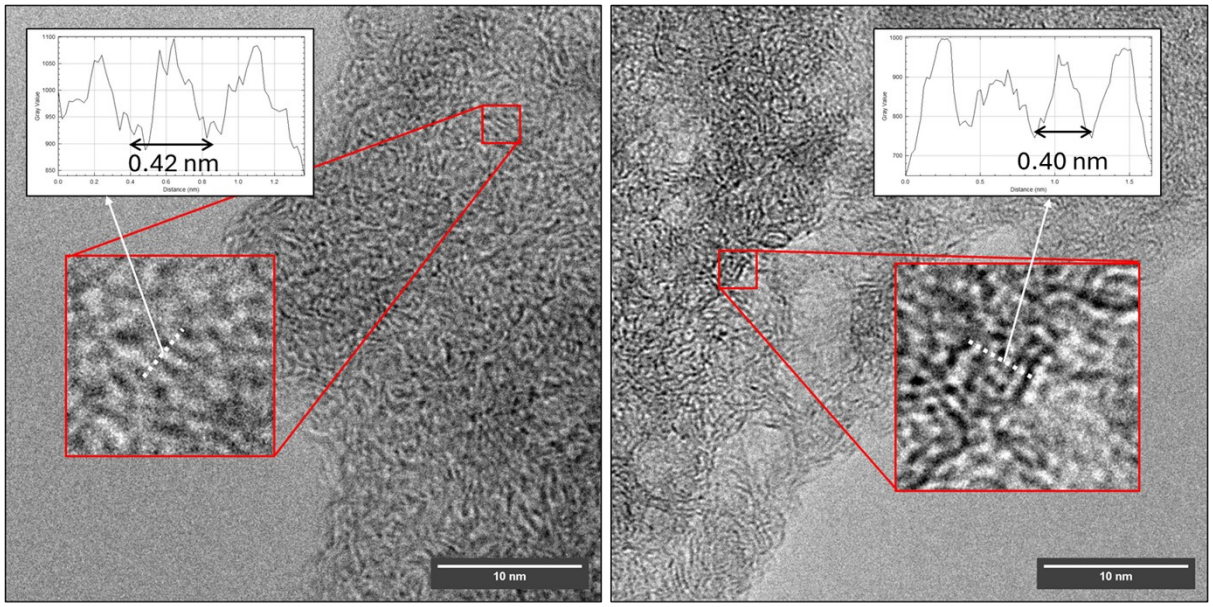

Figure S5 – TEM images of C400 (left) and C800 (right) at a magnification of x500k and profile plots of graphitic layers and interlayer distance.

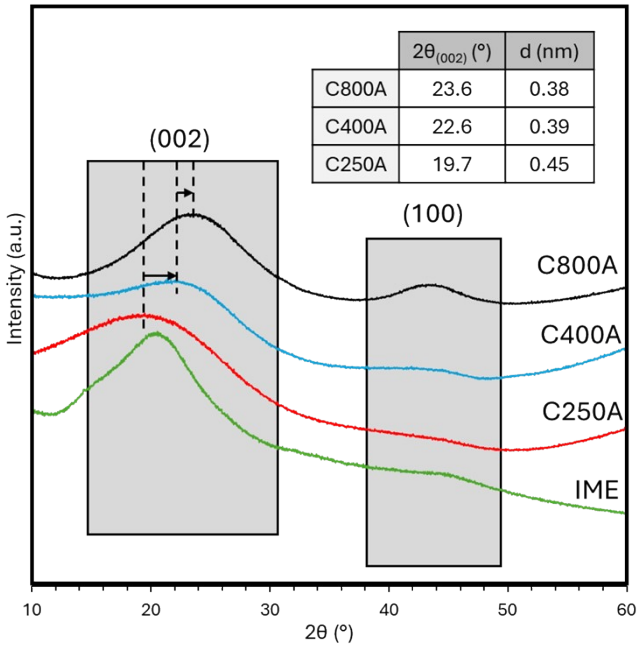

Figure S6 - pXRD diffractograms of **acid washed** carrageenan chars highlighting graphitic (002) and (100) diffraction planes and their respective d-spacing.

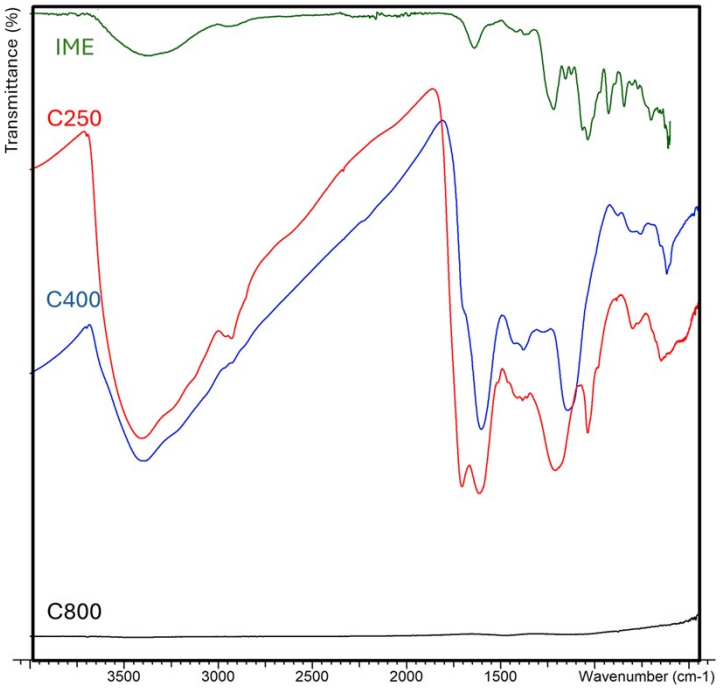

Figure S7 - FT-IR spectra (full range) of the initial carrageenan extract (IME) and subsequent chars, C250, C400, and C800.

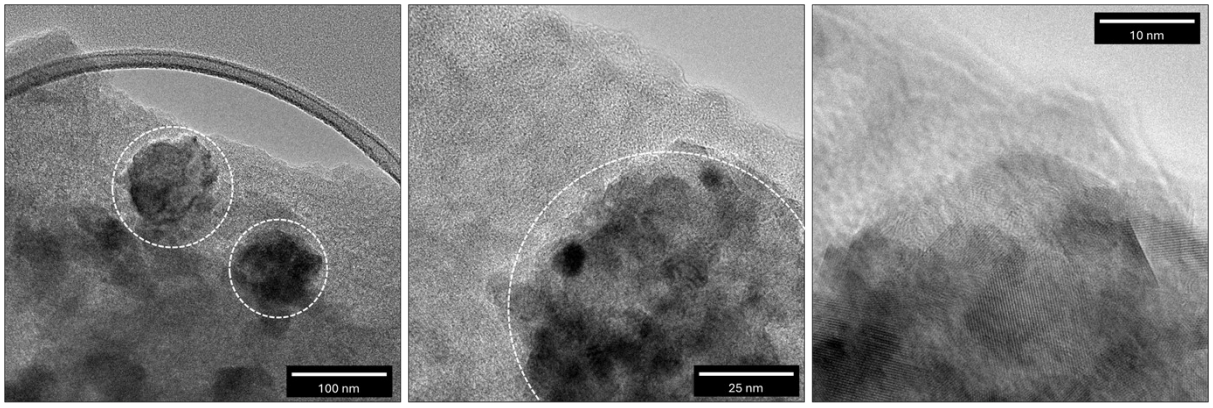

Figure S8 – TEM images of inorganic $Mg(OH)_2$ structures within C800 at magnifications of x50k (left), x200k (centre) and x500k (right).

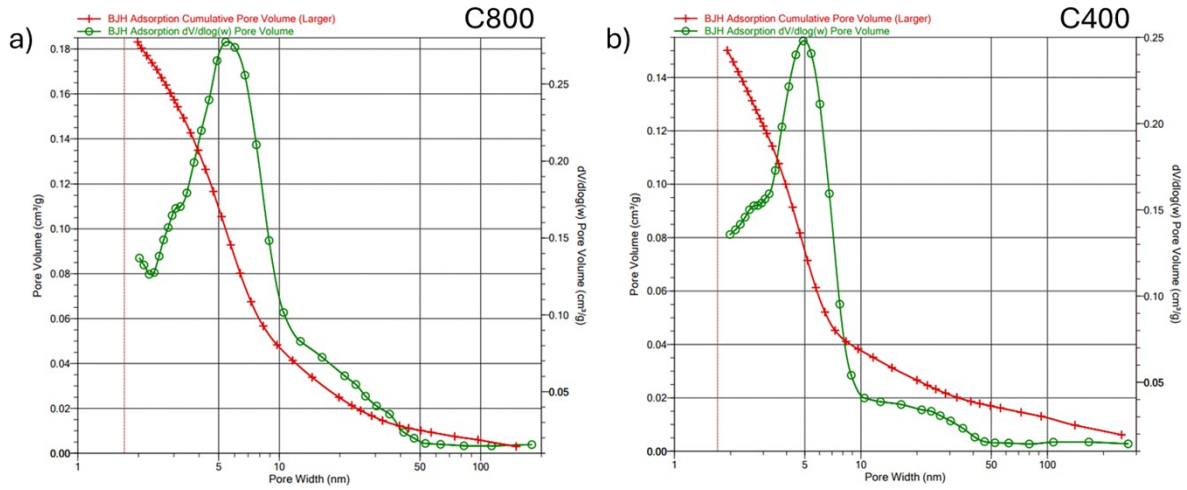

Figure S9 - BJH adsorption pore distributions of C800 and C400.

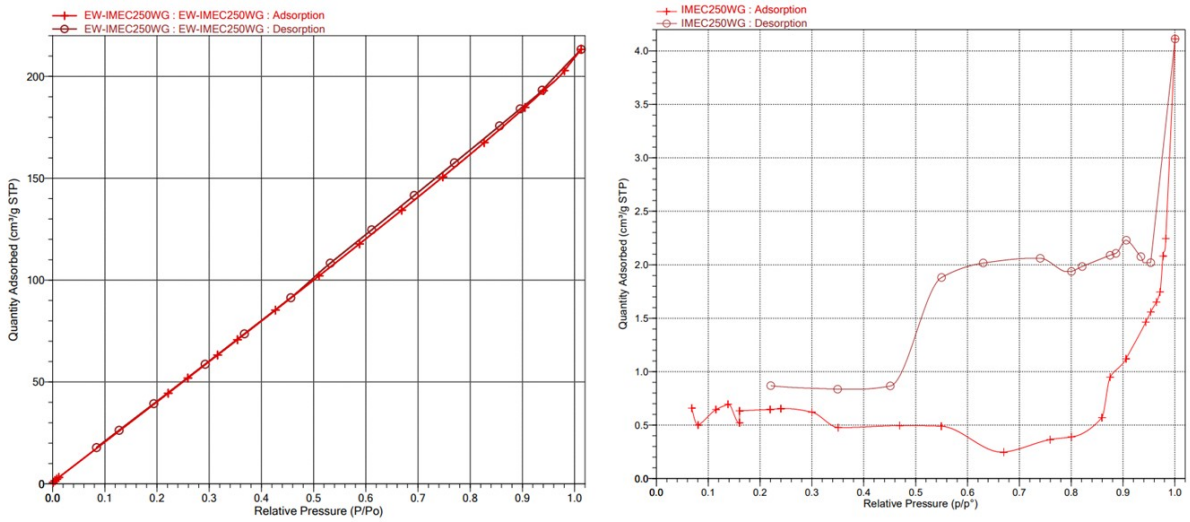

Figure S10 - N_2 adsorption porosimetry isotherms of C250.

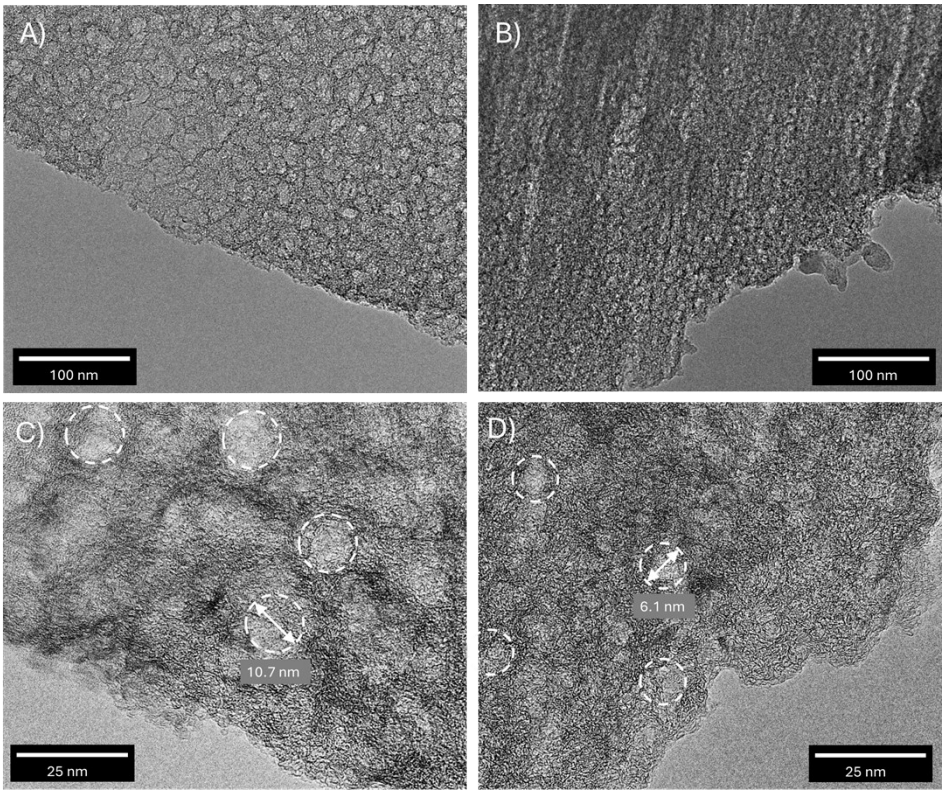

Figure S11 – TEM images of C800 at magnifications of x50k (A & B) and x200k (C & D) highlighting internal pore sizes.

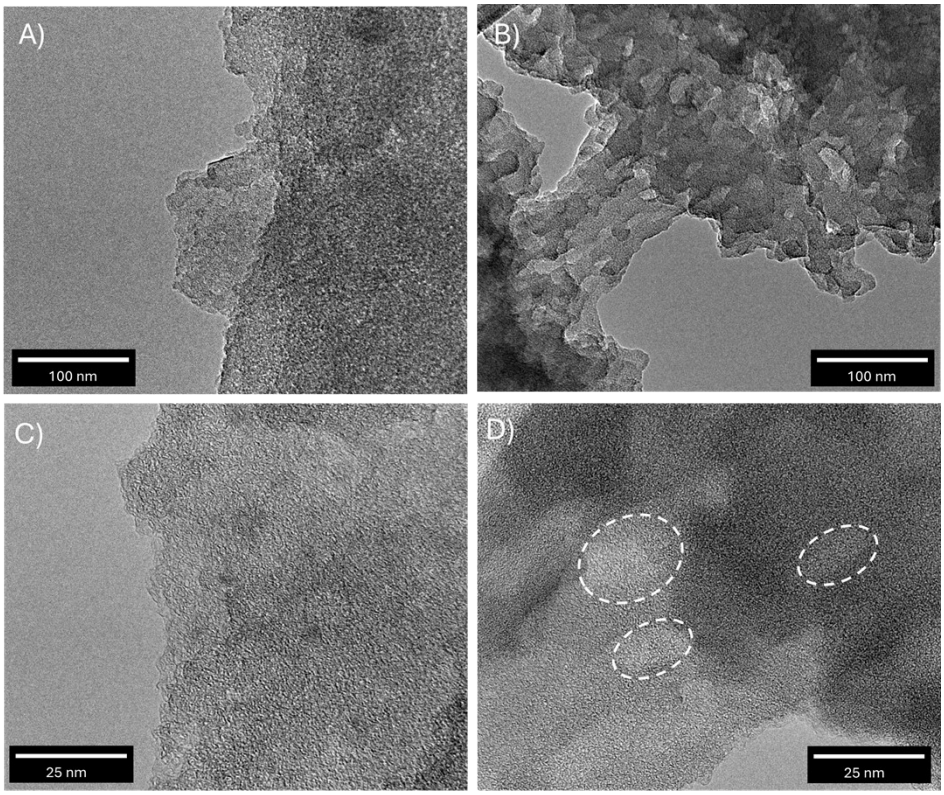

Figure S12 – TEM images of C400 (A & C) and C250 (B & D) at magnifications of x50k (A & B) and x200k (C & D) highlighting internal pore sizes.

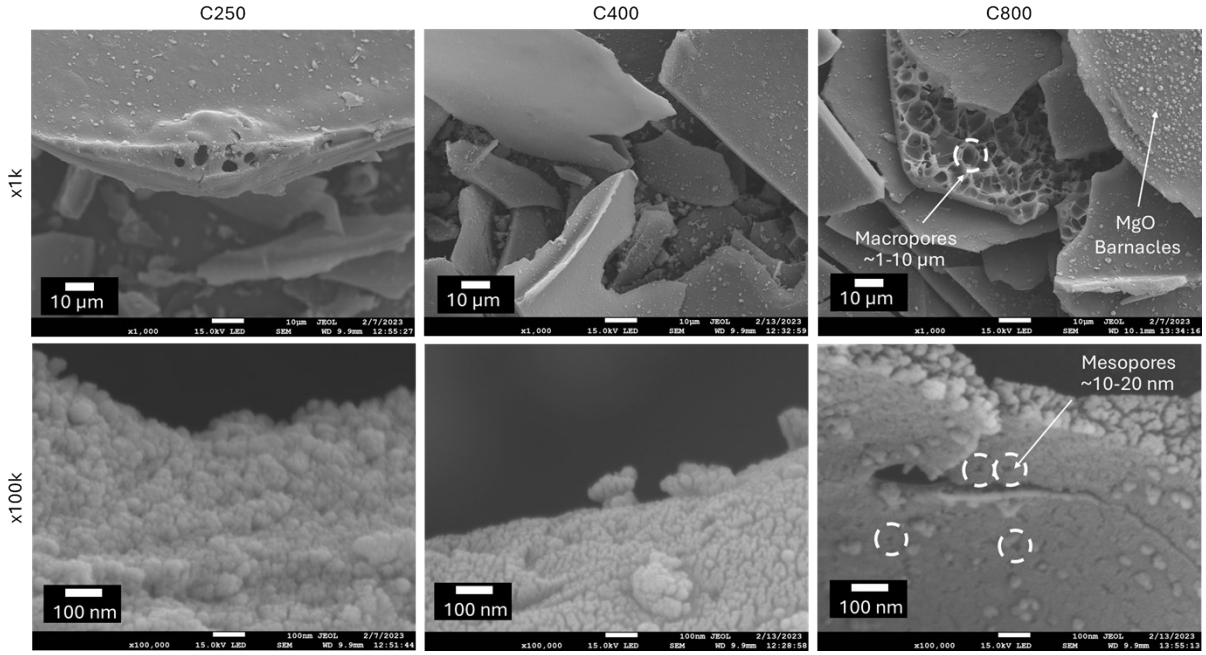

Figure S13 – SEM images of Pd/Au coated (5 nm) H_2O washed C250-C800 at magnifications of x1k and x100k.

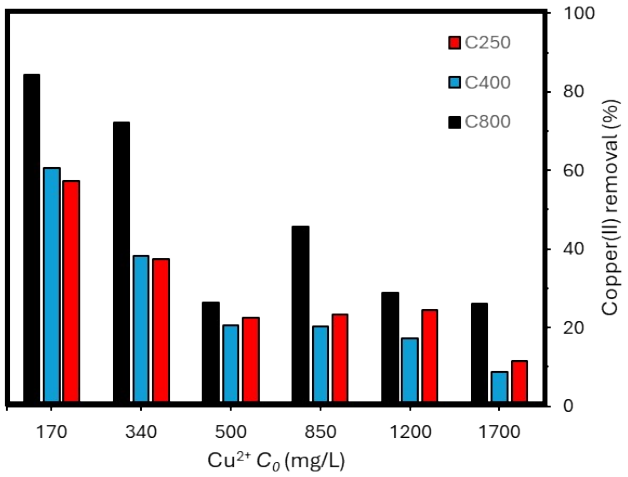

Figure S14 - Effect of initial copper(II) concentration (c_0) on the ability of C250-800 (5.0 mg/mL) to remove copper(II) from solution.

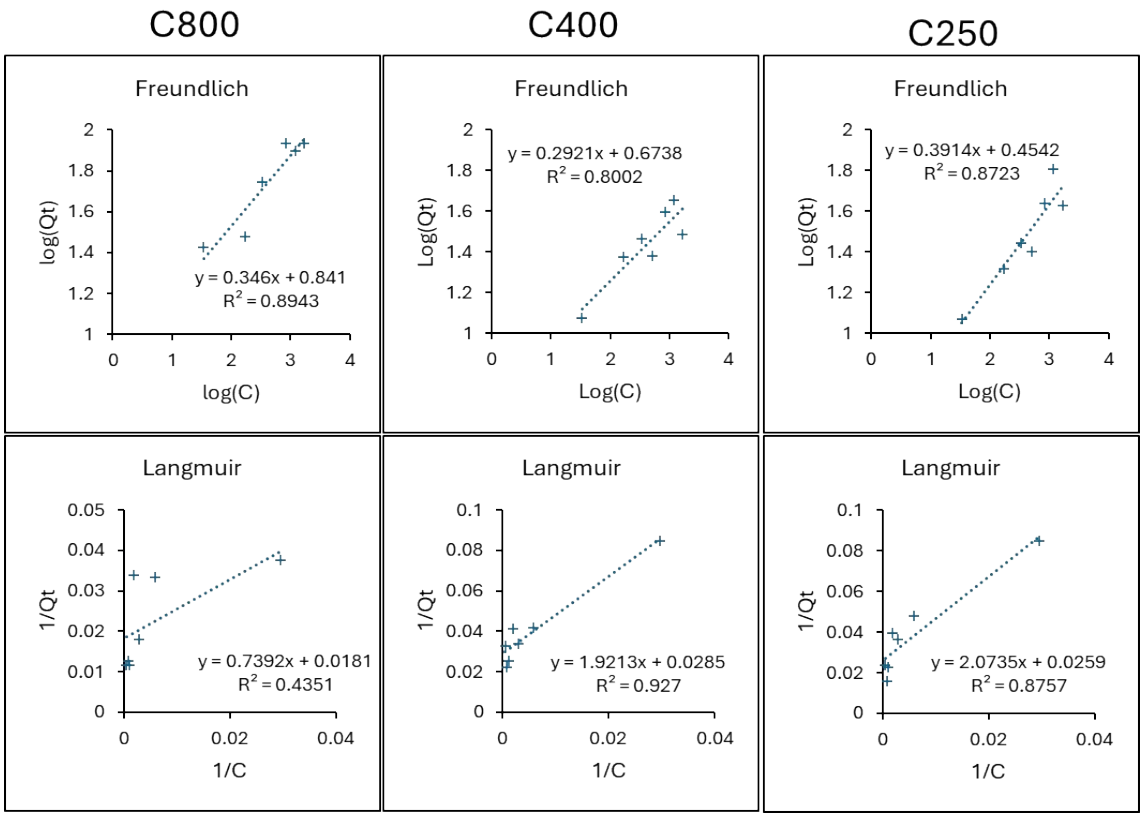

Figure S15 – Linearised Freundlich and Langmuir adsorption isotherm plots of copper(II) on C250-C800.

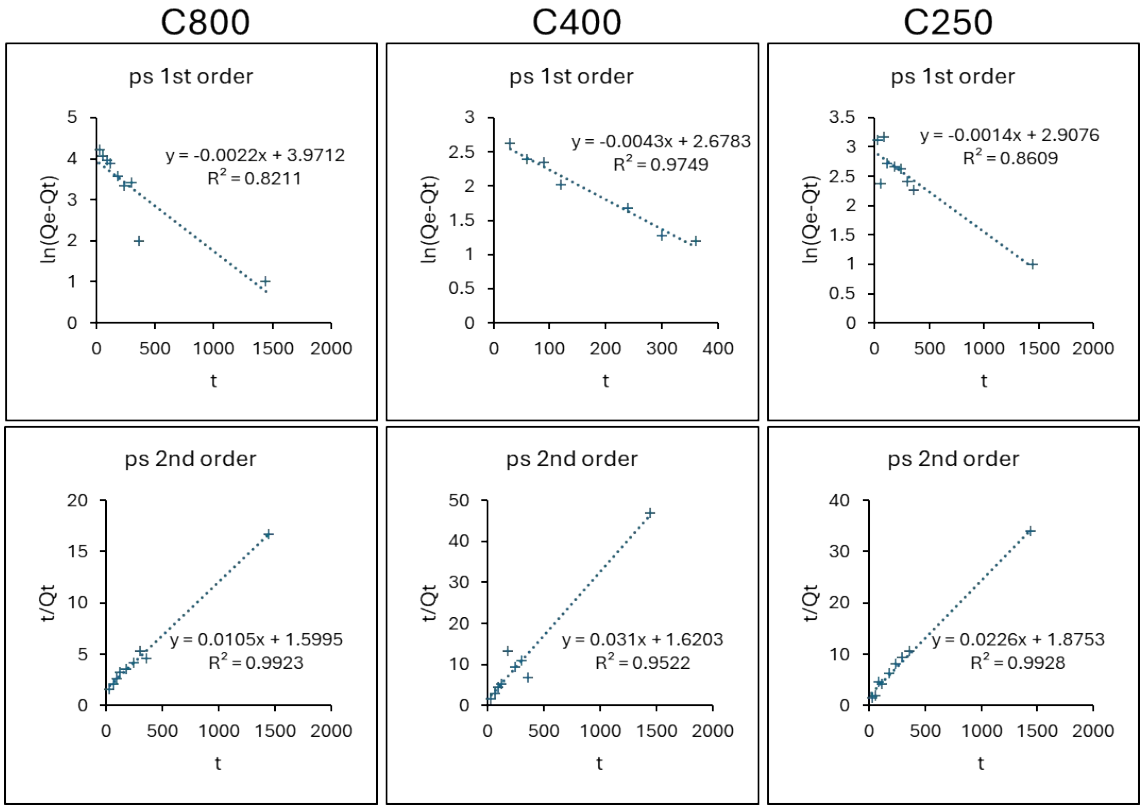

Figure S16 – Linearised pseudo-first and second kinetic model plots for the adsorption of copper(II) on C250-C800.

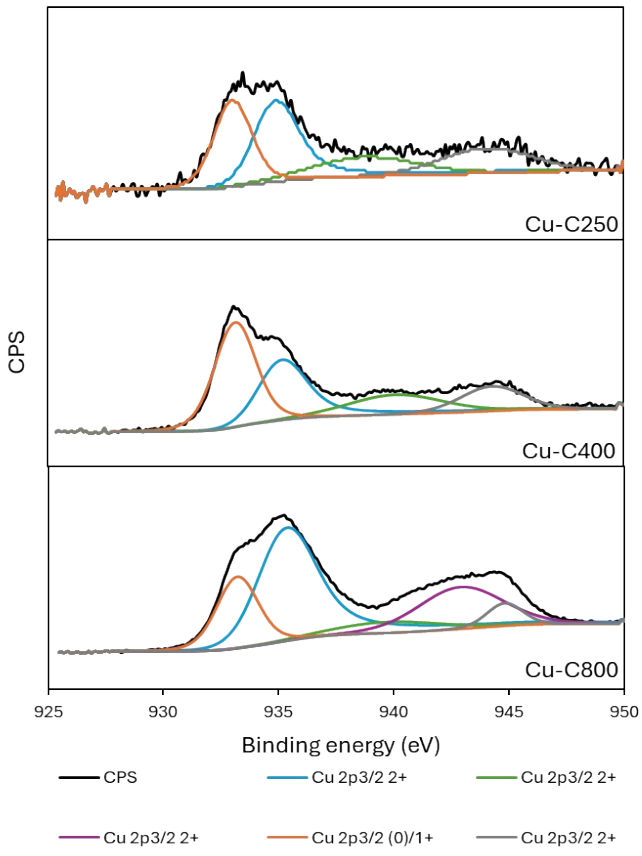

Figure S17 – Copper region (925-950 eV) XPS spectra of Cu-C(250-800) following adsorption (pH 4, c_0 1.7g/L, 24h, dosage 5 mg/mL)

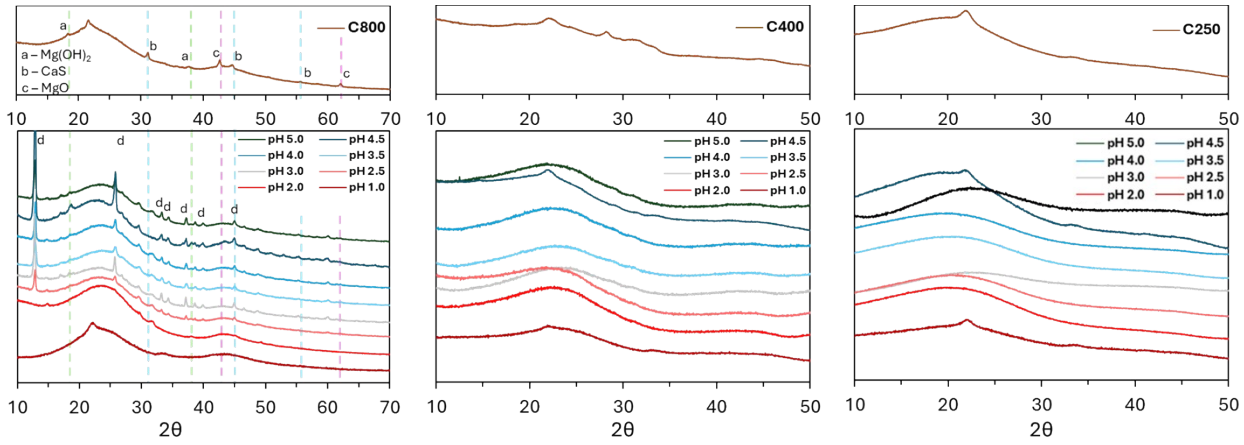

Figure S18 – pXRD diffractograms of Cu-C(250-800) at following adsorption at varying pH conditions (1.0-5.0) (c_0 1.3 g/L, 24h, dosage 5 mg/mL)

Supplementary tables

Table T1 - Elemental composition (CHNS and ICP-MS) of Carrageenan chars both washed (W = H_2O) and unwashed (U).

Material		Elemental Analysis % (Dry Weight)								
		C	H	N	S	O *	Mg	Ca	Na	K
IME		25.4 ±0.05	4.3 ±0.01	N.D	5.0 ±0.17	61.0	0.6	0.4	1.9	1.6
C250	U	39.3 ±0.04	1.8 ±0.03	N.D	7.5 ±0.18	-	-	-	-	-
	W	53.9 ±0.06	3.4 ±0.06	N.D	7.6 ±0.07	34.2	0.2	0.3	0.2	0.3
C400	U	46.2 ±0.07	2.5 ±0.04	N.D	3.49 ±0.09	-	-	-	-	-
	W	59.4 ±0.05	1.2 ±0.06	N.D	3.9 ±0.12	30.7	1.0	0.8	1.3	1.7
C800	U	51.1 ±0.12	0.38 ±0.05	N.D	3.7 ±0.08	-	-	-	-	-
	W	62.9 ±0.18	0.8 ±0.07	N.D	4.3 ±0.15	28.3	2.0	1.1	0.2	0.4

Table T2 - Surface area and pore properties (N_2 adsorption porosimetry) of carrageenan chars both washed (W = H_2O, A = 1M HCl) and unwashed (U).

Material		Surface area and pore properties		
		SA_{BET} (m^2/g)	V_{BJH} (cm^3/g)	APD (nm)
IME		0.37	0.012	20.9
C250	U	-	-	-
	W	-	-	-
	A	-	-	-
C400	U	0.3	0.002	69.8
	W	250	0.15	4.8
	A	510	0.21	4.5
C800	U	44	0.05	6.1

	W	290	0.18	5.3
	A	460	0.19	4.6

Table T3 - Isotherm model constants and errors determined for the adsorption of copper(II) to carrageenan chars (C250-800) at a pH of 4.0.

Material	Langmuir Isotherm					Freundlich Isotherm				
	K_L (L/mg)	q_m (mg/g)	R^2	χ^2	ERRSQ	K_F (L/mg)	$\frac{1}{n}$	R^2	χ^2	ERRSQ
C250	0.0125	38.6	0.876	19.22	1010.3	2.85	0.391	0.872	10.37	528.0
C400	0.0148	35.1	0.927	6.76	252.1	4.72	0.292	0.800	7.85	256.0
C800	0.00298	87.0	0.435	43.36	1882.5	6.93	0.346	0.894	38.06	1285.7

Table T4 - Kinetic parameters determined for the adsorption of copper(II) to carrageenan chars (C250-800) at a pH of 4.0.

Material	q_e (mg/g) (q_t , $t = 24h$)	Pseudo-first order				Pseudo-second order				
		K_1 (min^{-1})	R^2	χ^2	ERRSQ	q_e (mg/g)	K_2 (g mg^{-1} min^{-1})	R^2	χ^2	ERRSQ
C250	43.27	0.0019	0.821	88.97	2480.9	44.24	0.00030	0.993	11.24	312.8
C400	30.72	0.0047	0.975	43.34	1327.0	32.26	0.00065	0.952	23.00	815.7
C800	86.24	0.0033	0.861	27.69	1117.4	95.24	0.000084	0.992	5.57	376.2

References

1 J. Shannon, PhD Thesis, University of York, 2019

2 D. J. Shaw, in *Introduction to Colloid and Surface Chemistry*, Butterworth & Co., London, 2nd Edition, 1970, pp.133-166

3 N. Ayawei, A. N. Ebelegi and D. Wankasi, *J. Chem.*, 2017, **2017**, 1–11.

4 S. Kalam, S. A. Abu-Khamsin, M. S. Kamal and S. Patil, *ACS Omega*, 2021, **6**, 32342–32348

5 J.-P. Simonin, *Chem. Eng. J.*, 2016, **300**, 254–263.